

STRUCTURE OF METAL ADLAYERS DURING THE COURSE OF ELECTROCATALYTIC REACTIONS: O₂ REDUCTION ON Au(111) WITH Tl ADLAYERS IN ACID SOLUTIONS

R. R. ADŽIĆ,*† J. WANG† and B. M. OCKO‡

†Department of Applied Science, Chemical Sciences Division and ‡Department of Physics, Brookhaven National Laboratory, Upton, NY 11973, U.S.A.

(Received 30 March 1994)

Abstract—Surface X-ray scattering has been used to determine the structure of Tl adlayers on the Au(111) electrode surface during the course of O₂ reduction in acid solution. O₂ reduction is considerably catalyzed by Tl adlayers on Au(111). The half-wave potential is shifted to more positive values in the presence of the Tl adlayer. In the potential region between -0.18 and -0.4 V (vs. *sce*), the reaction mechanism changes from a 2e-reduction on Au(111) to a 4e-reduction on Au(111) covered with a low-coverage Tl phase. The close-packed rotated-hexagonal Tl phase, which exists in the potential range between -0.4 V and the bulk Tl deposition at ~ -0.7 V, has a lower activity for O₂ reduction than the low-coverage phase. O₂ reduction does not change the Tl coverage in this phase but causes a significant decrease of the in-plane diffracted intensity. This observation indicates that the O₂ molecules interact directly with the Tl adatoms prior to the charge transfer. It provides the most direct evidence that the outer sphere charge transfer mechanism is not operative for some surfaces. H₂O₂ reduction is facile on the surface covered with the low-coverage Tl phase, while it is almost completely suppressed by the rotated-hexagonal phase.

Key words: oxygen reduction, Au(111), thallium adatoms, X-ray scattering, adlayer structures

INTRODUCTION

The atomic structure of reaction sites is of exceptional importance for the areas of catalysis and electrocatalysis. Reliable information on the structure of these sites must be obtained *in situ*, *ie* during the course of the reaction. Recent advances in the *in situ* applications of surface X-ray scattering (SXS)[1, 2], scanning tunneling microscopy (STM)[3, 4] and atomic force microscopy AFM[5] have provided detailed information on the structures and phase transition behaviors of metal adlayers obtained by underpotential deposition (*upd*) and on the behavior of intrinsic (*eg*, bare) surfaces. In the area of electrocatalysis, therefore, it appears possible to identify the structure of active sites for a particular reaction since these techniques are capable of providing information on an atomic level on the structure of electrode surface.

Oxygen reduction on electrode surfaces is strongly influenced by foreign metal adatoms deposited at underpotentials. The *upd* species of Pb, Tl, Bi can considerably enhance the kinetics of O₂ reduction on Au. In the case of O₂ reduction on Au in alkaline solutions, a change in the mechanism from a 2e-reduction to a 4e-reduction was found with adlayers of the above atoms[6]. These effects are of fundamental interest in developing an understanding of the relationship of O₂ electrocatalysis to surface properties. Kinetic and mechanistic information, for

polycrystalline surface modified by a Tl adlayer in alkaline solution, have been obtained from rotating disk-ring measurements[7]. These same effects have been confirmed with single crystal electrodes[8]. The electrochemical data, however, do not provide information on the structure of the foreign metal adlayers which cause catalytic effects.

Metal adlayer structures have been related to electrocatalytic activity for H₂O₂ reduction on Au(111) with Bi(5) and Pb(9) adlayers using AFM in the absence of the electrocatalytic reaction. For the reaction on Au(111) in the presence of Bi adlayer, the active phase was identified as a primitive (2 × 2) Bi adlattice, while in the case of Pb, it was concluded that the adlayer of lead islands with high coverage is active for H₂O₂ reduction. A direct determination of the active structure for O₂ reduction on Au(100), during the course of the reaction, was attempted with the STM technique[10]. It was found that the active structure, facilitating a 4e-reduction, is unreconstructed Au(100) with the (1 × 1) symmetry, covered by chemisorbed partially discharged AuOH⁽¹⁻²⁾⁻ species.§

There are technical difficulties in deducing structures during the course of electrocatalytic reactions. In the case of SXS they originate from the construction of the cell which only has a 10–20 μm thick solution layer in contact with the surface of interest.

§ A direct observation of the surface structure by STM during the course of O₂ reduction may be unreliable due to the hindrance of the reaction by the tip, as discussed below.

* Author to whom correspondence should be addressed.

A depletion of a reactant from solution layer, because of an insufficient supply of the reactant by diffusion from the bulk solution, can complicate the structure determination during the course of the reaction. This is not a limitation for O₂ reduction, however, since it diffuses through a thin Prolene film covering the cell perpendicular to the whole surface investigated.

In the case of STM, or AFM the thin layer geometry may actually impede reactions. The tip and the electrode surface form a thin layer cell. The usual tip curvature radius of about 50 nm [11] is considerably larger than the area which can be imaged with the atomic resolution, for example 5 × 5 nm. Considering these dimensions, with the distance of the tip from the surface, ~10 Å, and that the only supply of the reactants is from the bulk solution by diffusion, it is likely that the tip can block the access of the reactant to the surface being imaged. Some differences between the X-ray diffraction and STM data have been ascribed to the limited supply of the reactant to the area under the tip [12]. The effect of the tip on the supply of the reacting species has been also observed in the bulk deposition of Cu on the Au(111) and Au(100) electrode surfaces [13].

The effects of Tl adlayers on O₂ reduction on gold surfaces in acid solution have not been previously investigated with electrochemical methods. Gold is a poor catalyst in acid solution and the reaction proceeds only with the exchange of two electrons, with H₂O₂ as the reaction product [14]. In this work, electrochemical, and X-ray scattering techniques were used to establish the effect of Tl on O₂ reduction kinetics and to determine structural characteristics during the course of O₂ reduction on Au(111). A hanging meniscus rotating disk electrode was used to determine the effects of the Tl adlayer on O₂ and H₂O₂ reduction. Significant catalytic effects of adsorbed Tl have been found. The half-wave potential of a 2e-reduction is shifted to more positive potentials, a 4e-reduction occurs at less positive potentials which partly reverts back to a 2e-reduction at high Tl coverages. Here we show that the structure which facilitates a 4e-reduction of O₂ and reduction of H₂O₂ originates from the low-coverage Tl phase. The close-packed rotated-hexagonal phase is the structure causing the inhibition of H₂O₂ reduction and a partial reversal of the O₂ reduction mechanism to a 2e-reduction. This phase is stable in the presence of O₂. It gives, however, a considerably smaller diffracted intensity at a low-order Tl wavevector and we interpret this in terms of an increase of the lateral Tl disorder in the presence of O₂ reduction. The intensity decrease is a consequence of the O₂-Tl interaction during the course of O₂ reduction. This shows that the adsorption of O₂ takes place before the charge transfer and resolves a longstanding question whether the reaction involves the outer sphere charge transfer mechanism, see *eg* Ref. [13] and references therein.

EXPERIMENTAL

A gold disk (2 by 10 mm diameter) was aligned and polished as previously reported [2]. The angle between the optical plane and the [111] crystallo-

graphic planes was measured to be 0.15°. After sputtering and flame annealing, the sample was protected by pure water and transferred through air into an electrochemical X-ray scattering cell constructed from Kel-F [2]. The cell was sealed using a 4 μm-thick Prolene (Chemplex) X-ray window. An outer cell could be filled with flowing high purity nitrogen gas to prevent oxygen diffusing through the Prolene film. In the measurements of O₂ reduction the outer cell was opened to air. The solutions were prepared from TiNO₃ (Aldrich) dissolved in HClO₄, HClO₄ (Merck) and Milipore QC water (Milipore Inc.). After deoxygenation with nitrogen gas, the solution was injected into the cell. At a potential slightly positive of the bulk Tl deposition potential, the cell was deflated which leaves a thin 10 μm-thick capillary electrolyte film between the Au(111) face and the Prolene X-ray window. A Ag/AgCl (3 M KCl) electrode was used as a reference electrode. In order to minimize the chloride leakage to the cell, the reference electrode was separated by two frits with 0.1 M HClO₄ solution between them. The potentials are given with respect to saturated calomel electrode (*sce*).

Rotating hanging meniscus electrode measurements were carried out with a crystal 6 mm in diameter, 6 mm long, prepared by the flame annealing method. The rotator (Pine Instrument Co.) was fitted with a collet crystal holder which is similar to the one described earlier [15].

Surface X-ray scattering can be used to prove surface structure within the surface plane or along the surface normal direction by controlling the direction of the scattering vector **Q**, which is the difference between the incident and scattered X-ray wave vectors [1, 2]. Typically, information within the surface plane is obtained by orienting **Q** almost entirely within the surface plane. This corresponds to the grazing incident angle geometry. When **Q** is directly aligned along the surface normal direction (specular reflectivity) information is obtained about surface normal structure. On the other hand, when **Q** has fixed in-plane component equal to an allowed reflection of the substrate (non-specular reflectivity), the intensity distribution depends on both the surface normal structure and the registry of the electrodeposited adlayer with respect to the underlying substrate lattice.

SXS measurements were carried out at the National Synchrotron Light Source (NSLS) at beam line X22B with $\lambda = 1.54 \text{ \AA}$. A full description of the electrochemical SXS technique has been presented elsewhere [2]. For Au(111) it is convenient to use a hexagonal coordinate system in which $\mathbf{Q} = (a^*, b^*, c^*) \cdot (H, K, L)$, where $a^* = b^* = 4\pi/\sqrt{3}a = 2.25 \text{ \AA}^{-1}$, $c^* = 2\pi/\sqrt{6}a = 0.89 \text{ \AA}^{-1}$, and $a = 2.885 \text{ \AA}$. The in-plane diffraction measurements were carried out in the (H, K) plane with $L = 0.2$ corresponding to a grazing angle of 1.25°.

RESULTS AND DISCUSSION

Voltammetry of upd of Tl on Au(111) in HClO₄ solution

Figure 1 shows a linear potential voltammetry curve for the upd of Tl on Au(111) in 0.1 M HClO₄

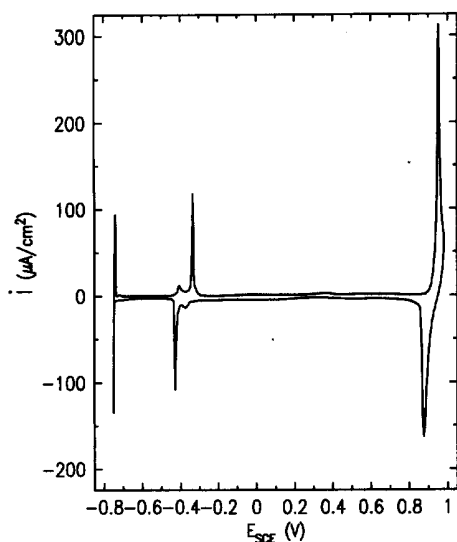


Fig. 1. Voltammetry curve for the *upd* of Tl on Au(111) in 0.1M HClO₄ containing 5mM TlNO₃; sweep rate 20mVs⁻¹.

containing 5 mM Tl⁺. Two pronounced peaks in the anodic sweep occur at -0.45 and -0.37 V. Besides these well defined peaks, the Tl adsorption occurs over a wide potential region between the bulk Tl deposition and the large anodic peak at 0.92 V. This adsorption, as in alkaline solution[16], causes a small increase of the current and the appearance of small broad peaks. The charge associated with the anodic peaks at -0.45 and -0.37 V corresponds approximately to 0.35 of a gold monolayer, which is the same as the charge associated with the cathodic peaks at about -0.40 and -0.48 V. The actual Tl coverage, determined by SXS, in the potential range between -0.45 and -0.7 V changes from 0.70 to 0.75 monolayer with decreasing potential. This suggests that an additional 0.35 monolayer of Tl is deposited at potentials between -0.35 and 0.9 V. The calculation of the charge associated with the *upd* of Tl at $E > -0.35$ V is difficult because of the necessity for *a priori* separation of the double layer charging and the faradaic adsorption. This subtraction causes considerable errors when the double layer charging and faradaic currents are of similar magnitude, or when the *upd* occurs in the whole accessible potential range, as in this case.

The unusual peak at 0.92 V appears to be associated with the surface process involving the Tl⁺/Tl³⁺ redox reaction. The chemical nature of this species, and its relation to the Tl adlayer at more negative potentials, will be the subject of a future communication.

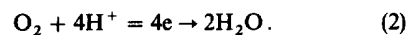
Oxygen reduction

It has been shown previously that Tl adlayers cause considerable catalytic effects on O₂ reduction on gold surfaces in alkaline solutions[7, 8]. There are however, no reports on the effects of Tl adlayer on the reaction in acid solutions. The reduction of O₂ on gold in acid solutions proceeds with the

exchange of two electrons[17], *ie*,



This reaction on Au(111) is kinetically hindered and, due to very slow kinetics, the diffusion limiting current density is not reached before hydrogen evolution commences. In this work, a rotating hanging meniscus Au(111) disc electrode was used to obtain kinetic information on O₂ reduction on the Au(111) electrode in acid solution in the presence of a Tl adlayer. Figure 2 shows polarization curves, at several rotation rates, for O₂ reduction on Au(111) covered with a Tl adlayer in 0.1M HClO₄ with 5mM Tl⁺ and on Au(111) without Tl. The presence of adsorbed thallium causes pronounced catalytic effects. The reaction is shifted to more positive potentials in the presence of Tl adsorbates, and in the potential region from about -0.15 to 0.2V it proceeds with the exchange of two electrons. At more negative potentials, as the Tl coverage increases, the reaction proceeds with the exchange of four electrons. The overall reaction can be written in the following way:



This can be inferred from the application of Levich's equation[18] to the data from Fig. 2, *viz.*,

$$i_D = 0.62nFAD_0^{2/3}\omega^{1/2}\nu^{-1/6}C_0 \quad (3)$$

where i_D is the diffusion limiting current density, n is the number of electrons exchanged in O₂ reduction, A is the electrode surface area, D_0 is the O₂ diffusion coefficient, ω is the rotation rate, ν is the kinematic viscosity and C_0 is the bulk concentration of O₂.

The insert in Fig. 2 shows a factor of two difference in the slope of the plot of the diffusion limiting current density as a function of $\omega^{1/2}$ for a 4e-reduction at the cathodic current maximum than for a 2e-process at $E = -0.15$ V. A good agreement

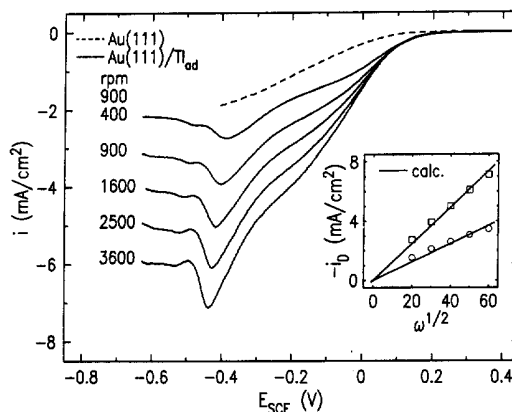


Fig. 2. Polarization curves for O₂ reduction on the rotating hanging meniscus Au(111) electrode in 0.1M HClO₄ containing 5mM TlNO₃. Dashed line gives the curve for Au(111) without Tl. Rotation rate is given in the graph; sweep rate is 20mVs⁻¹. The insert shows the i_D vs. $\omega^{1/2}$ plots at -0.15 V (circles) and at the cathodic current maximum (squares), and the plots calculated for $n = 4$ and $n = 2$ using Levich's equation (see the text).

between the calculated and experimental curve for a 4e-reduction is obtained. For O_2 , the values $D_0 = 1.93 \times 10^{-5} \text{ cm}^2 \text{ s}^{-1}$ and $C_0 = 1.22 \times 10^{-6} \text{ mol cm}^{-3}$ and the solution kinematic viscosity, $\nu = 9.13 \times 10^{-3} \text{ cm}^2 \text{ s}^{-1}$ were used in calculations[19]. The fact that the O_2 reduction in acid solution, on a poor catalyst such as gold, can be catalyzed to proceed as a 4e-reaction on the Au(111) surface in the presence of a low-coverage Tl adlayer, is an important finding for oxygen electrocatalysis. Surprisingly, at more negative potentials, *ie*, at higher overpotentials for O_2 reduction, in the region of higher Tl coverage, the reaction partly reverts back to a 2e-process. A partial, rather than a complete reversal of O_2 reduction to a 2e-reaction, may be due to the flux of O_2 from the gas phase into the hanging meniscus which appears to be considerable in this potential region.

The shift of the cathodic current maximum to more negative potentials with increasing rotation rate is mostly due to the potential drop on an uncompensated solution resistance in the layer between the Luggin capillary and the electrode surface. Traces of some adventitious impurities can contribute to this effect by shifting the *upd* of Tl to more negative potentials.

Additional information on the effects of Tl on O_2 kinetics, especially on the question of the change from a 2e- to 4e-reduction, can be obtained from the measurements of H_2O_2 reduction. Figure 3 shows a comparison of O_2 and H_2O_2 reduction on Au(111) in the presence of Tl. The reduction of H_2O_2 coincides with the potential region of a 4e-reduction of O_2 . At potentials negative to the principle *upd* peak for Tl, the reaction seems to be almost completely blocked. In the same potential region, O_2 reduction partially reverts back to a 2e-reduction. The coincidence of a 4e-reduction of O_2 and the reduction of H_2O_2 suggests a series mechanism of O_2 reduction on Tl-modified Au(111), *ie*, the reaction path prob-

ably involves H_2O_2 as the intermediate. The mechanistic aspects of this reaction are outside the scope of this paper.

SXS measurements

Grazing incident angle X-ray diffraction measurements were performed in order to determine the surface structure of electrodeposited thallium adlayers during the course of O_2 reduction. In the absence of Tl adsorption and O_2 reduction, the in-plane diffraction pattern from the unreconstructed Au(111) surface is composed of only the integer reflections which are shown as solid circles in Fig. 4a. The presence of an electrodeposited Tl adlayer gives rise to a rotated hexagonal diffraction pattern in the potential region from -0.7 to -0.45 V in 0.1 M $HClO_4$ with 5 mM Tl^+ . This rotated-hexagonal phase has also been observed in alkaline solution[15]. The angle Ω represents the angle by which the diffraction pattern is rotated from the low-index gold reflections. The magnitude of the lowest order in-plane wavevector gives the Tl reciprocal lattice constant, τ . Both τ and Ω vary with potential. The real space lattice constant $a_{Tl} = 4\pi/\tau\sqrt{3}$ and the Tl coverage, θ , in relation to the gold surface density is equal to $(a_{Au}/a_{Tl})^2 = (\tau/a_{Au}^*)^2$. At all potentials, the Tl lattice is incommensurate with the gold substrate and the rotation angle, Ω , ranges from 5 to 6.5°. Figure 4b shows the real-

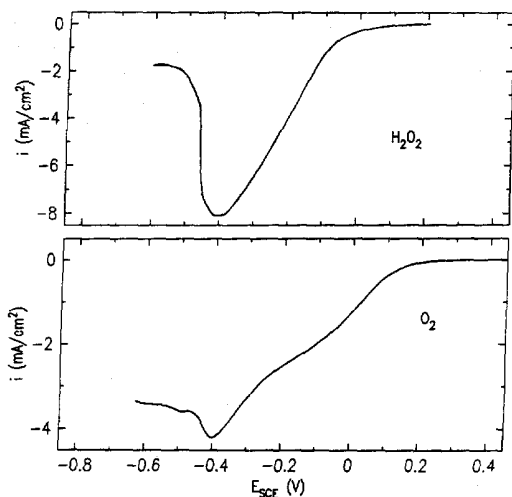


Fig. 3. Polarization curves for H_2O_2 (upper panel) and O_2 (lower panel) reduction on the rotating hanging meniscus Au(111) electrode in 0.1 M $HClO_4$ containing 5 mM $TlNO_3$. Rotation rate 900 rpm; H_2O_2 concentration: 8 mM; sweep rate 20 mV s^{-1} .

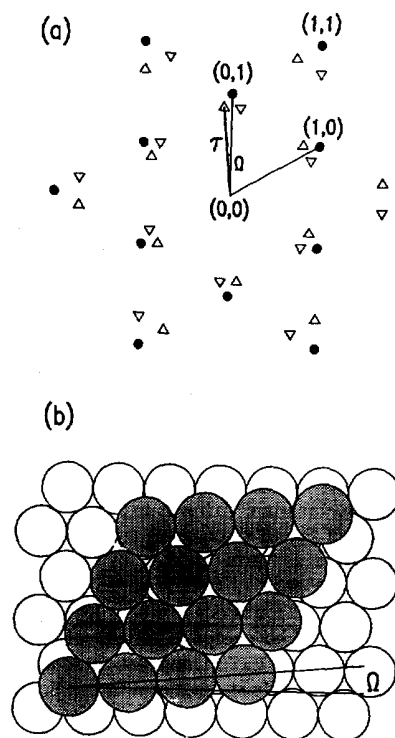


Fig. 4. (a) The in-plane diffraction pattern for Au(111)/Tl at -0.65 V in 0.1 M $HClO_4$ with 5 mM $TlNO_3$. Solid circles represent the diffraction pattern from the Au(111) substrate. The triangles and inverted triangles represent the diffraction pattern from the Tl monolayer from the two symmetry equivalent domains of the rotated-hexagonal phase. (b) Real-space model of the rotated-hexagonal Tl monolayer deduced from (a).

space model of this rotated-hexagonal Tl phase on Au(111).

The low-order Tl diffraction peak position and intensity were monitored as a function of potential in the range from -0.70 to -0.46 V. Radial scans, shown in Fig. 5a, illustrate how the diffraction peak position (defined as τ) and intensity vary with potential. At all potentials, the diffraction peaks are well described by Lorentzian profiles, shown as solid lines. The Tl-Tl separation and coverage calculated from τ are plotted in Fig. 6a and b, respectively. Within this phase the Tl-Tl separation is close to its bulk value of 3.432 Å. The Tl coverage equals 0.743 monolayer just prior to bulk deposition. The integrated X-ray intensity shown in Fig. 6c starts to decrease at the potential of the first anodic current peak (-0.45 V) and drops sharply over the second anodic peak (-0.37 V). The diffraction from the rotated-hexagonal phase completely vanishes above -0.35 V.

In the presence of O₂, during the course of its reduction, the rotated-hexagonal phase is preserved. Figure 5b shows radial scans similar to those shown in Fig. 5a, but taken with the X-ray window exposed to air. Oxygen penetrates the thin film and is reduced as the sample surface giving rise to a significant cathodic current. Despite a large decrease of the scattered intensity (note there is a factor of ten decrease of the intensity scale from Fig. 5a and b), the rotated-hexagonal Tl monolayer structure remains. The Tl coverage, calculated from τ , is practically unchanged, however, the peak width increases by approximately 30%. In addition, the fact that the X-ray specular reflectivity spectra (not shown) do not show a significant difference with or without oxygen reduction suggests that the Tl coverage remains the same. Thus, we can rule out a partial desorption of Tl as a possible cause of the decrease in the intensity

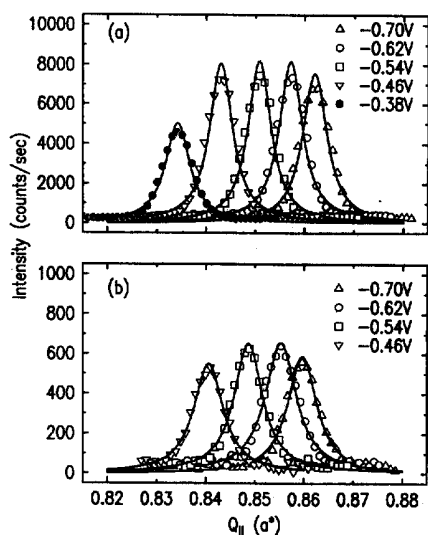


Fig. 5. (a) Radial scans through one of the low-order diffraction peaks of the Tl monolayer on Au(111) in 0.1 M HClO₄ with 5 mM TlNO₃ in the rotated-hexagonal phase as a function of potential. (b) Same measurements as in (a) but in the presence of O₂ reduction.

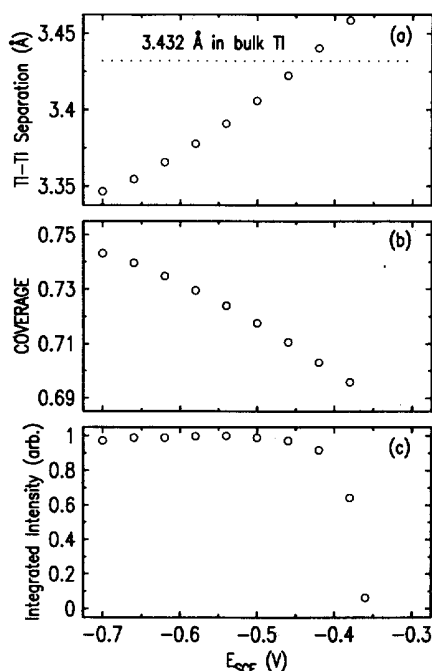


Fig. 6. The Tl-Tl separation (a) and the coverage (b) of the rotated-hexagonal phase of Tl on Au obtained from Fig. 5(a) and normalized integrated intensity of the radial scans (c) as a function of potential.

with O₂. For this peak, the integrated intensity (over both in-plane directions) decreases by about 80% after the O₂ is turned on. The effect of oxygen can be interpreted in terms of an increase in the lateral disorder of the Tl monolayer. The intensity completely recovers within several minutes after the oxygen in the outer cell is replaced by nitrogen. These results show that oxygen interacts directly with the Tl adatoms and provides direct evidence that the outer sphere charge transfer mechanism is not operative.

In order to obtain additional information on the Tl adlayer, especially at potentials where an ordered phase does not appear to exist, the potential dependence of the intensity at the non-specular position (0, 1, 0.5) was measured in the absence of O₂. This reciprocal space position is sensitive to the registry of the Tl adatoms with respect to the underlying gold lattice [1, 20]. As a function of potential, rapid changes in the non-specular intensity provide a simple means of delineating the phase boundary of the electrodeposited adlayer phases. In Fig. 7a we show the scattered intensity at (0, 1, 0.5) in the positive potential sweep. After background subtraction, the intensity has been normalized to unity at its maximum. Within the rotated-hexagonal phase there is a small positive slope, followed by a sharp intensity decrease at about -0.4 V. This coincides with the vanishing of the phase and the sharp peaks in the voltammetry curve (Fig. 7b). The potential of the maximum in the cathodic current, due to a 4e-reduction, is shifted to somewhat more negative potentials because of the potential drop on the uncompensated solution resistance, as discussed in the section on O₂ reduction. A gradual increase of

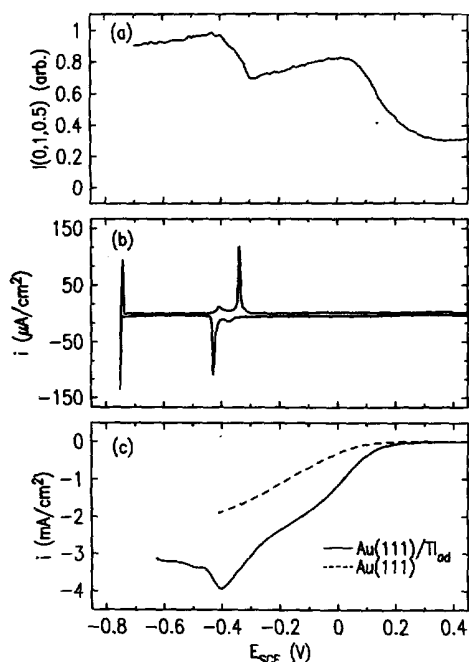


Fig. 7. Normalized scattered intensity at (0, 1, 0.5) for Au(111) in the presence of Tl as a function of potential change in the positive sweep at 1 mV s^{-1} (a). Voltammogram curve (adapted from Fig. 1) (b) and polarization reduction (identical to Fig. 2) curve for O_2 given for comparison (c).

scattered intensity between -0.35 and 0.0 V is observed, followed by a decrease at more positive potentials to the plateau at 0.4 V . This supports the observation from voltammogram curves that the Tl adsorbate is present on the surface above -0.35 V and that the coverage decreases with increasing potential over the range -0.35 – 0.4 V . In alkaline solution, the coadsorption of OH^- facilitates the ordering of Tl at low coverage[15]. An aligned-hexagonal phase forms at potential between -0.4 and -0.2 V where the Tl coverage is around 0.5. Within this potential region, the aligned hexagonal phase and possible phases which are aligned along the $\langle 10 \rangle$ and $\langle 11 \rangle$ symmetry axes were not observed. It is difficult to rule out short range of Tl adlayer since it is difficult to observe broad peaks due to the large diffuse background from the window and electrolyte.

Although the exact coverage and structure of the Tl adlayer at potentials between -0.35 and -0.15 V cannot be determined in this study, the finding that the low-coverage Tl phase catalyzes a 4e-reduction of O_2 (see Fig. 7c) is significant. A similar catalytic effect has previously been found in alkaline solution in the presence of an ordered Tl adlayer with coadsorbed OH^- [12]. The fact that the 4e-reduction of O_2 occurs in both cases indicates that the reaction is facilitated by the low coverage of Tl and is not particularly dependent on the structural details. In the close-packed rotated-hexagonal phase, the Tl adatoms appear completely discharged, as found for alkaline solution[15]. Therefore, the close-packing and neutral atomic state of Tl is not conducive to a 4e-reduction. The catalytic effect of the low coverage

Tl phase can be attributed to, either the effect of the interaction of O_2 with a partial Tl adlayer, or some partial charge remaining on the Tl adsorbate. The former allows O_2 or H_2O_2 to bond in bridging configuration between Au and Tl atoms which can facilitate the break of the O–O bond. The latter increases the possibility of Tl adsorbates to interact with the intermediates in oxygen reduction.

CONCLUSIONS

The data presented above illustrate the unique possibility of the SXS technique for determining the structure of electrode surfaces during the course of electrochemical reactions. Some limitations of the mass transport, caused by a thin layer cell geometry, may, for fast reactions make the identification of the surface structure more difficult. It appears, however, that these limitations can be overcome with an adequate design of the experiment and reliable structure-activity correlations can be established.

O_2 reduction on Au(111) is considerably catalyzed by Tl adlayers. The onset of the reaction is shifted to more positive potential. In the potential region from about -0.15 to 0.20 V , the reaction proceeds as a 2e-process on the surface covered by a low coverage of disordered Tl adsorbate. In the potential range from about -0.4 to -0.18 V , the reaction mechanism changes from a 2e-reduction. In this potential region the surface is covered by a low coverage Tl phase whose ordering could not be established by X-ray diffraction. The rotated-hexagonal Tl phase, which exists in the potential range between -0.4 V and the bulk Tl deposition, has a lower activity for O_2 reduction than the low-coverage phase, facilitating partially a 2e-process. O_2 reduction causes a five-fold decrease of the diffracted intensity at a low-order hexagonal diffraction peak. The Tl coverage appears, however, unchanged.

Hydrogen peroxide reduction is facile on the surface covered with the low coverage Tl phase, while it is almost completely suppressed by the rotated-hexagonal phase. No reduction was observed at potentials positive to the existence of the low coverage Tl phase.

The model describing the O_2 –Tl/Au interaction can be only speculative at this moment. The decrease of the diffracted intensity for the close-packed rotated-hexagonal phase during O_2 reduction shows that O_2 interacts directly with Tl adlayer prior to the charge transfer. This means that the outer-sphere charge transfer mechanism is not operative in this reaction on some surfaces.

Acknowledgements—The authors thank O. Magnussen, W. Polewska and S. Feldberg for useful discussions. This research was performed under the auspices of the US Department of Energy, Division of Chemical Sciences and Materials Sciences Division, Office of Basic Energy Sciences under Contract No. DE-AC02-76CH00016.

REFERENCES

1. M. F. Toney, J. G. Gordon, G. M. Samant, G. L. Borges, D. G. Wiesler, D. Yee and L. B. Sorensen, *Langmuir* 7, 796 (1991).

2. J. Wang, B. M. Ocko, A. J. Davenport and H. S. Isaacs, *Phys. Rev.* **B46**, 10321 (1992); B. M. Ocko, J. Wang, A. J. Davenport and H. S. Isaacs, *Phys. Rev. Lett.* **65**, 1466 (1990).
3. O. M. Magnussen, J. Holtos, R. J. Nichols, D. M. Kolb and R. J. Behm, *J. vac. Sci. Technol.* **B9**, 969 (1991).
4. X. Gao, A. Hamelin and M. J. Weaver, *Phys. Rev.* **B46**, 7096 (1992); X. Gao, A. Hamelin and M. J. Weaver, *J. chem. Phys.* **95**, 6993 (1991).
5. C.-H. Chen, A. A. Gewirth, *J. Am. chem. Soc.* **114**, 5439 (1992).
6. R. R. Adzic, In *Advances in Electrochemistry and Electrochemical Engineering* (Edited by H. Gerischer and C. Tobias). J. Wiley and Sons, New York (1984).
7. R. Amadelli, N. Markovic, R. Adzic and E. Yeager, *J. electroanal. Chem.* **159**, 391 (1983).
8. R. R. Adzic, N. M. Markovic and A. V. Tripkovic, *J. electroanal. Chem.* **150**, 79 (1983).
9. C. Chen, N. Washburn and A. A. Gewirth, *J. phys. Chem.* **97**, 9754 (1993).
10. W. Polewska, C. M. Vitus, B. M. Ocko and R. R. Adzic, *J. electroanal. Chem.* **364**, 265 (1994).
11. C. J. Chen, *Introduction to Scanning Tunneling Microscopy*. Oxford University Press, Oxford (1993).
12. J. Wang, O. M. Magnussen, B. M. Ocko and R. R. Adzic. Unpublished
13. R. J. Nichols, D. M. Kolb and R. J. Behm, *J. electroanal. Chem.* **313**, 109 (1991).
14. E. B. Yeager, *J. Mol. Catal.* **38**, 5 (1986).
15. B. D. Cahan and H. M. Villulas, *J. electroanal. Chem.* **307**, 263 (1991).
16. J. Wang, R. R. Adzic and B. M. Ocko, *J. phys. Chem.* Submitted for publication.
17. A. Zwetanova and K. Juttner, *J. electroanal. Chem.* **119**, 149 (1981); S. Strbac and R. R. Adzic, *J. Serbian chem. Soc.* **57**, 835 (1992).
18. V. G. Levich, *Physicochemical Hydrodynamics*. Prentice-Hall, Englewood Cliffs (1962).
19. J. Zagal, P. Bindra and E. Yeager, *J. electrochem. Soc.* **127**, 1506 (1980).
20. B. M. Ocko, G. M. Watson and J. Wang, *J. phys. Chem.* **98**, 897 (1994).